



OPEN

Differential mast cell numbers and characteristics in human tuberculosis pulmonary lesions

Karen Magdalena Garcia-Rodriguez^{1,2}, Estela Isabel Bini³, Armando Gamboa-Domínguez³, Clara Inés Espitia-Pinzón⁴, Sara Huerta-Yepey⁶, Silvia Bulfone-Paus^{1,2,5} & Rogelio Hernández-Pando³✉

Tuberculosis (TB) is still a major worldwide health threat and primarily a lung disease. The innate immune response against *Mycobacterium tuberculosis* (*Mtb*) is orchestrated by dendritic cells, macrophages, neutrophils, natural killer cells and apparently mast cells (MCs). MCs are located at mucosal sites including the lungs and contribute in host-defence against pathogens, but little is known about their role during *Mtb* infection. This study investigates the location and characteristics of MCs in TB lesions to assess their contribution to TB pathology. To this purpose, number, location and phenotype of MCs was studied in 11 necropsies of pulmonary TB and 3 necropsies of non-TB infected lungs that were used as controls. MCs were localised at pneumonic areas, in the granuloma periphery and particularly abundant in fibrotic tissue. Furthermore, MCs displayed intracellular *Mtb* and IL-17A and TGF- β immunostaining. These findings were validated by analysing, post-mortem lung tissue microarrays from 44 individuals with pulmonary TB and 25 control subjects. In affected lungs, increased numbers of MCs expressing intracellularly both tryptase and chymase were found at fibrotic sites. Altogether, our data suggest that MCs are recruited at the inflammatory site and that actively produce immune mediators such as proteases and TGF- β that may be contributing to late fibrosis in TB lesions.

Abbreviations

MCs	Mast cells
TB	Tuberculosis
MC _T	Mast cells expressing tryptase
MC _C	Mast cells expressing chymase
MC _{TC}	Mast cells expressing both tryptase and chymase
<i>Mtb</i>	<i>Mycobacterium tuberculosis</i>
DC	Dendritic cells
NK cells	Natural killer cells

Tuberculosis (TB) caused by *Mycobacterium tuberculosis* (*Mtb*), remains one of the deadliest bacterial infections worldwide¹. During infection, *Mtb* reaches the lungs where different innate immune cells reside including mast cells (MCs)^{2–4}. *Mtb* is phagocytosed by macrophages leading to the release of diverse cytokines, including TNF α and IL-6 that drive the inflammatory process⁵. To control *Mtb* spread, innate and adaptive immune cells surround infected phagocytic cells promoting granuloma formation^{5,6}. The cytokines IL-17A and TNF- α are known to contribute to the process⁷. When granuloma containment fails, different lung injuries including pneumonia, bronchitis, caseous necrosis and eventually fibrosis prevail^{8,9}. The fibrotic process in human lungs has been associated with the presence of TGF- β , and the proteases, tryptase and chymase^{10,11}. The final TB pathology

¹Lydia Becker Institute of Immunology and Inflammation, Faculty of Biology, Medicine and Health, University of Manchester, Manchester, UK. ²Manchester Collaborative Centre for Inflammation Research, Faculty of Biology, Medicine and Health, University of Manchester, Manchester, UK. ³Seccion de Patologia Experimental, Instituto Nacional de Ciencias Medicas y Nutricion "Salvador Zubiran", Mexico City, Mexico. ⁴Departamento de Inmunologia, Instituto de Investigaciones Biomedicas, Universidad Nacional Autonoma de Mexico, Mexico City, Mexico. ⁵Division of Musculoskeletal and Dermatological Sciences, Faculty of Biology, Medicine and Health, University of Manchester, Manchester, UK. ⁶Unidad de Investigacion en Enfermedades Oncologicas, Hospital Infantil de Mexico, Federico Gomez, Mexico City, Mexico. ✉email: rhdezpando@hotmail.com

phase culminates in irreversible lung tissue damage manifested by necrosis and fibrosis^{8,9}. Although many cells are involved in this process, little is known about the contribution of MCs in this pathology.

MCs are distributed in lungs and mucosal tissues and contribute to host-defence against bacterial infections¹². In humans, MCs are classified as tryptase + MCs (MC_T), chymase + MCs (MC_C) or both tryptase + and chymase + MCs (MC_{TC})¹³. Upon bacterial exposure, they release a wide variety of cytokines and chemokines, including IL-17, TNF- α , IL-8 and TGF- β either by degranulation or canonical secretory pathways¹⁴. Additionally, during lung infections MCs are altered in numbers, phenotype and localization^{15,16}. For instance, MC numbers are decreased in lungs of *Streptococcus pneumoniae* infected patients¹⁷. Furthermore, MCs are capable to phagocytose bacteria and present antigens¹⁸. Although hypothetically MCs have an important role in TB³, little has been explored. For instance, it is unknown if MCs are localized at pulmonary tuberculous human lesions and what is the predominant MC phenotype. It is also unclear whether MC cytokines, e.g. IL-17A, and TGF- β contribute to the inflammatory process, and formation and maintenance of granulomas and fibrogenesis.

In this study we examined number, distribution and phenotype of MCs in human TB-infected lungs and MC cytokine expression at granulomas and fibrotic sites in TB-infected lung tissue. Our descriptive findings demonstrated that MCs are likely to participate to the early inflammatory phase, as well as to the late fibrosis formation during TB pathology.

Materials and methods

Ethical statement and tissue procurement. All methods were performed in accordance to relevant guidelines and regulations. Lung tissue sections from 11 necropsies of deceased TB patients and 3 controls from non-TB infected necropsies were obtained from the Pathology Department files at the National Institute of Medical Sciences and Nutrition “Salvador Zubiran” in Mexico City. A specific informed consent was not required for this study, but every medical autopsy was performed with a signed authorization of the representative legal family member and tissue samples were obtained during legally authorized autopsies with signed permission by a relative who agreed tissue sample donation for the present and previous studies¹⁹. The microarray tissue study from 44 individuals with pulmonary TB and 25 control subjects were taken from the Pathology Department of the General Hospital of Mexico ‘Eduardo Liceaga’ at Mexico City, and ethical statement was approved by the local ethic committee of the Hospital Infantil de Mexico, Federico Gomez (No. HIM/2008/015). This study including all experimental protocols were approved by the in-house ethical committee at the National Institute of Medical Sciences and Nutrition “Salvador Zubiran”.

TB tissue processing. Macroscopically, lung tissue from 11 necropsies of deceased TB patients showed extensive cavitory bilateral lung disease, surrounded by numerous white nodules with irregular shapes and size that alternated with pneumonia patches. Extensive sampling was performed, obtaining several tissue fragments from different lesions and were embedded in paraffin blocks sectioned at 3 μ m and mounted in glass slides. Additionally, we used post-mortem lung tissue, essentially granulomas, from 44 individuals with pulmonary TB and 25 control subjects (subjects who died as a result of any other cause without significant pulmonary disease). The lung tissues (TB and control tissue samples) were organized in a tissue microarray (MTA) as previously described²⁰. One sample of each section (lung sections and MTA) were stained with haematoxylin and eosin (HE) to select lung lesions for study. Spare sections were left at room temperature before being used for immunoperoxidase and immunofluorescence staining. The lung tissues in this study correspond to active TB cases, not latent TB cases were included.

Immunoperoxidase staining. Lung sections were deparaffinized and treated with antigen retriever (1X; Bio SB, Santa Barbara, California) for 5 min under microwave heating. Endogenous peroxidase was blocked incubating tissue with methanol-H₂O₂ (9:1) for 10 min. After three washes, unspecific sites were blocked using a background sniper (BIOCARE MEDICAL; Pacheco, California) for 30 min. Slides were washed and incubated with either a rabbit anti-human chymase antibody (Ab186417, Abcam; Cambridge, United Kingdom) or a mouse anti-tryptase antibody (Ab2378, Abcam; Cambridge, United Kingdom) for 2 h. After three washes, tissue was processed using a mouse/rabbit PolyDetector DAB (3–3'-diaminobenzidine)/HRP (horseradish peroxidase) brown detection system (BSB0219, Bio SB; Santa Barbara, California) following manufacturer’s instructions. Micrographs were acquired using a LEICA DMLS microscope with a 2.5X and 40X dry objectives equipped with a LEICA DFC295 camera and analysed using an automated image analyser (QWin Leica; Wetzlar, Germany).

Immunofluorescence staining. To visualize MC phenotypes, lung tissue sections were deparaffinized, treated with DNA retriever (1X; Bio SB; Santa Barbara, California) for 5 min under heating and incubated with blocking buffer (goat serum 1:10 in PBS + tween 0.1%) for 30 min. After three washes, tissue were incubated with a rabbit anti-human chymase antibody (Ab186417, Abcam; Cambridge, United Kingdom), and a mouse anti-tryptase antibody (Ab2378, Abcam; Cambridge, United Kingdom) for 1 h followed by 1 h incubation with a goat anti-mouse antibody conjugated to Alexa 488 fluorophore (Ab150117, Abcam; Cambridge, United Kingdom) and a goat anti-rabbit antibody conjugated to Alexa 647 fluorophore (Ab150083, Abcam; Cambridge, United Kingdom). After three washes, tissue was mounted using a fluoroshield mounting media containing 4',6-diamidino-2-phenylindole (DAPI, Abcam; Cambridge, United Kingdom). Slides were analysed using a fluorescent microscope OlympusBX41 with either 40 \times and 10 \times dry objectives. Images were acquired using a Zen 2.6 blue and analysed using Fiji.

To analyse cytokine expression and *Mtb* internalization, lung sections were deparaffinized, treated with DNA retriever (1X; Bio SB; Santa Barbara, California) for 5 min under heating and incubated with blocking buffer (goat serum 1:10 in PBS + tween 0.1%) for 30 min. After three washes, tissues were incubated with a mouse

anti-tryptase antibody (Ab2378, Abcam, Cambridge, United Kingdom) and either a rabbit polyclonal anti-*Mtb* (CP140C, BioCare Medical), capable to recognize diverse *Mtb*-cell wall and secreted antigens, rabbit anti-TGF- β (Jackson ImmunoResearch, Cambridge, United Kingdom) or rabbit anti-IL-17 (SC7927 Santa Cruz Lab, USA) antibodies for 1 h followed by 1 h incubation with a goat anti-mouse antibody conjugated to either Alexa 488 (Ab150117, Abcam; Cambridge, United Kingdom) or Alexa 647 fluorophores (Ab150115, Abcam; Cambridge, United Kingdom) and a goat anti-rabbit antibody conjugated to either Alexa 647 (Ab150083, Abcam; Cambridge, United Kingdom) or Alexa 488 fluorophores (Ab150081, Abcam; Cambridge, United Kingdom). After three washes, tissue was mounted using a fluoroshield mounting media containing 4',6-diamidino-2-phenylindole (DAPI, Abcam; Cambridge, United Kingdom). Slides were analysed using a confocal microscope LSM 710 DUO, Carl Zeiss.

MC quantification. Forty-four MTAs from TB-infected lung sections from autopsy cases and 22 non-TB infected controls contained in 4 different slides were stained with HE and analysed. Five MTAs were selected as control lung tissue and 10 MTAs presenting fibrosis were selected as representative fibrotic tissue. Selected MTAs were immunostained with tryptase and chymase (as described above) and studied at 10 \times magnification using a fluorescent microscope Olympus BX41 and acquired using Zen 2.6 blue software system. One high power field was taken for each MTA and all single positive (MC_C or MC_T) and double positive (MC_{TC}) cells were counted per field using Fiji. MC numbers were graphed using GraphPrism.

Statistical analysis. A Shapiro–Wilk tests was performed to determine normality during phenotype quantification. Statistical analysis was achieved using Kruskal–Wallis test and a Dunn’s multiple comparison post-test (adjusted $p \leq 0.01$) using GraphPad Prism 8th edition.

Compliance with Ethical standards. Authors declare that no conflict of interest happened during the present study. The present research involved the use of lung sections obtained from deceased individuals. Autopsies were selected from the Pathology Department files at the National Institute of Medical Sciences and Nutrition “Salvador Zubiran” in Mexico City. A specific informed consent was not required for this study, but every medical autopsy was performed with a signed authorization of the representative legal family member and tissue samples were obtained during legally authorized autopsies with signed permission by a relative who agreed tissue sample donation for this and previous studies¹⁹. Additional tissue was obtained from the Pathology Department of the General Hospital of Mexico ‘Eduardo Liceaga’ at Mexico City, and ethical statement was approved by the local ethic committee of the Hospital Infantil de Mexico, Federico Gomez (No. HIM/2008/015).

Experimental procedures. All methods were performed in accordance to relevant guidelines and regulations. This study including all experimental protocols were approved by the in-house ethical committee at the National Institute of Medical Sciences and Nutrition “Salvador Zubiran”.

Results

Tryptase positive mast cells are the most abundant phenotype in non-TB infected human lungs. In physiological conditions MCs expressing either tryptase or chymase or both proteases reside in alveolar parenchyma. However, in pulmonary infections MC numbers and phenotype are altered²¹. To investigate lung MC distribution and their characteristics we studied their number, location and phenotype in autopsies from control lungs (non-TB infected). Control cases had heart attacks as death cause with lungs showing overall a normal structure with some focal patches of centrilobular emphysema (Fig. 1A). These tissues showed MC_T (Fig. 1B) and lesser MC_C (Fig. 1C) at alveolar walls. Both MC_T and MC_C were preferentially located in blood vessels adventitia. Moreover, MC_T were the most abundant phenotype (median = 5 cells per field) (Fig. 1D) followed by MC_{TC} (median = 2 cells per field), whereas MC_C were not detected. In fact, all MC_C observed were also tryptase + therefore MC_{TC} (Fig. 1E). Thus, MCs expressing only chymase were rare whereas tryptase positive MCs were predominant in human lung parenchyma.

Mast cells are located at active inflammatory sites of TB-infected lungs and show intracellular mycobacterial antigens.

MC numbers, location and phenotype found in non-infected lungs were used as controls to investigate MC characteristics in TB lung lesions. A table summarizing clinical data from the studied TB active necropsies is shown in Supplemental Table 1. Both MC phenotypes (MC_T and MC_C) were abundant at inflammatory (granulomas, pneumonia, vascular and airways walls) and fibrotic areas (Fig. 2), but absent in the proximity of necrotic sites (Supplemental Fig. 1). At pneumonic areas (Fig. 2A), numerous MCs were seen in alveolar walls and alveolar lumen (Fig. 2B,C), while in blood vessels (Fig. 2D) MCs were found in the adventitia and in bronchial airways (Fig. 2E,F). Both phenotypes were positioned below the epithelium, in the submucosa and in the muscular wall between smooth muscle cells. Furthermore, as shown in Fig. 2G, MC_T stationed in inflammatory regions of TB-infected lung sections showed vacuoles containing *Mtb* antigens. Thus, both MC_T and MC_C reside in TB lung lesions and store *Mtb*.

Mast cells are located at the periphery of granulomas and express IL-17. Granulomas are characterized by a necrotic core containing *Mtb* surrounded by macrophages and lymphocytes and a fibrotic external layer²⁰. As shown in Fig. 3, granulomas at different stages were analysed. In early or incipient granulomas (Fig. 3A), characterized by small nodular congregates of inflammatory cells, occasional MCs were seen intermixed with lymphocytes and macrophages (Fig. 3B,C). However, MCs were not observed to infiltrate typical or

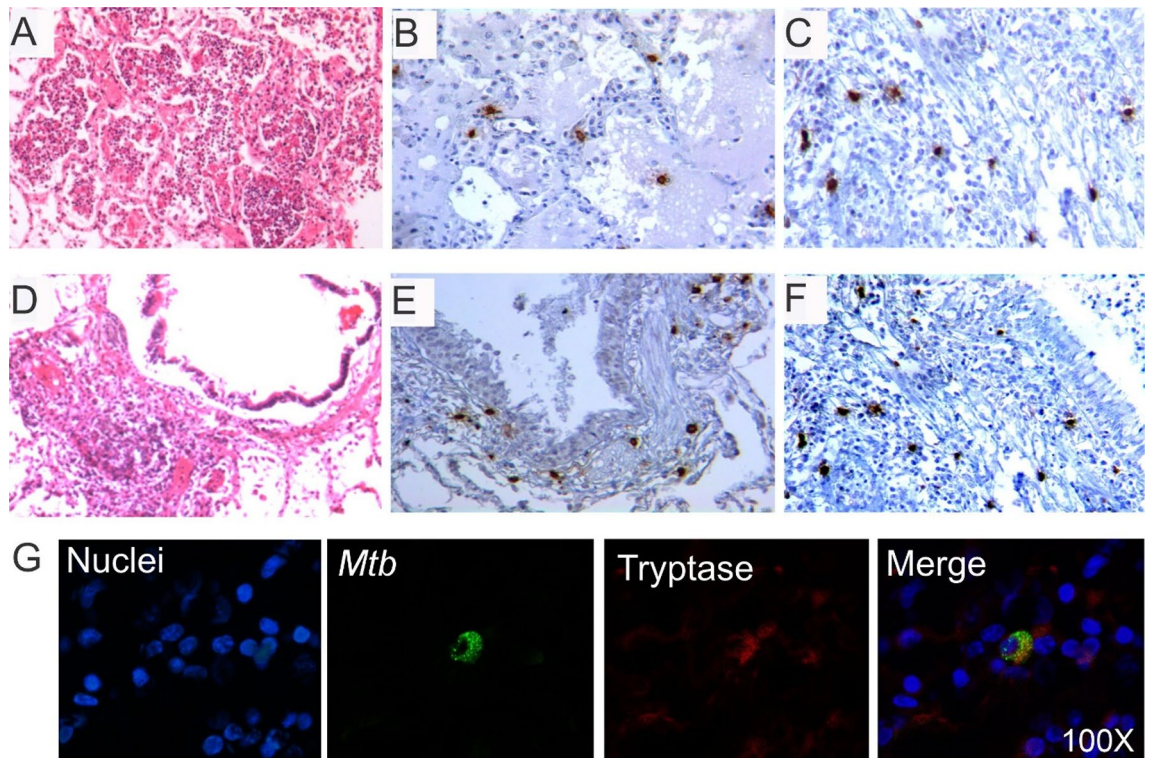


Figure 2. Tryptase and chymase positive mast cells are located at active inflammatory lesions and show intracellular mycobacterial antigens. (A) Representative HE micrograph showing areas of tuberculous pneumonia. (B) Tryptase + MCs are present in alveolar walls and lumen. (C) Chymase + MCs show similar numbers and distribution as tryptase + MCs in the pneumonic areas. (D) Extensive inflammatory infiltrate is detected in bronchial walls. (E) Numerous tryptase + MCs are located in the bronchial submucosa. (F) Numerous chymase + MCs are in bronchial walls and neighbour alveoli. Micrographs are representative of 11 necropsies of TB patients. (G) A representative section with extensive inflammation in pneumonic areas was incubated with polyclonal anti-*Mtb* (Alexa 488 label) and anti-tryptase antibodies (Alexa 647 label). High power micrograph shows a MC expressing tryptase that colocalize with *Mtb* antigens.

Our observations in lung controls showing MCs surrounding blood vessels and throughout the alveolar-capillary interstitial tissue with MC_T as the most abundant population are in line with current evidence that shows MC_T as predominant phenotype in large airways including bronchial and alveolar, followed by MC_{TC} which are more common at blood vessels, whereas MC_C are rare or sporadically observed in human lungs^{24,25}. Although it is not clearly understood yet, this suggests that MC_T reside in the alveolar parenchyma prone to activation or differentiation upon environmental stimulus¹⁶.

Since MCs release a wide variety of cytokines, chemokines and antimicrobial molecules, they are likely to be involved in TB pathogenesis at different stages³. For instance, since our findings show that MCs locate at inflammatory areas of TB-infected human lungs, here MCs may contribute to the initial TB inflammatory stage by releasing TNF- α , IL-6, MCP-1, IL-1 β , GM-CSF and IL-8. Muñoz et al. support this concept by showing the release of MC-dependent TNF and IL-6 upon *Mtb* infection^{26,27}. Furthermore, the ability of MCs to contribute to immune cell recruitment was observed in *Chlamydia pneumoniae* lung infection characterised by a MC-dependent cellular infiltration in the lung airways^{12,28–30}. Instead, the appearance of MCs at incipient granulomas and surrounding mature granulomas suggests their contribution in orchestrating granuloma formation and maintenance potentially by the secretion of IL-17, IL-6, IL-8, MCP-1, IL-10, IFN- γ and IL-1 β ^{31,32}. However, MC mediators including TGF- β , IL-33, chymase and IL-1 β are known to induce excessive inflammation and fibrosis and have detrimental effects³¹. Thus, suppressing MC-mediators release, e.g. IL-1 β and TGF- β may diminish MC activation³³ as proposed in SARS-COV2 infection^{34,35} and serve to prevent TB fibrosis.

In our study, we observe that human-lung resident MCs display intracellular *Mtb* fragments. This is in line with reported data^{26,27} showing MCs able to uptake *Mtb* via membrane binding through lipid rafts and CD48 receptor engagement²⁷. Although MCs are not professional phagocytic cells, they are known to phagocytose³⁶ and kill bacteria via acidified vacuoles³⁷. These findings would support the role of MCs in uptaking and eliminating *Mtb* through phagocytosis or serve as a reservoir of intracellular *Mtb* during the active phase of TB infection. Although is not within the scope of this study, further research is needed to investigate whether MCs contribute to T cell activation as described in other conditions^{36,38,39} via *Mtb*-antigen presentation.

Mtb persistence promotes an ongoing cellular recruitment⁴⁰ that results in the formation of early granulomas^{6,40}. The association between MCs and TB-induced granulomas is still controversial. A positive correlation between MCs and granuloma formation was observed in tuberculous lymphadenitis tissue⁴¹ but not in tuberculous liver tissue⁴². Our data demonstrate that MCs infiltrate incipient granulomas and locate at the

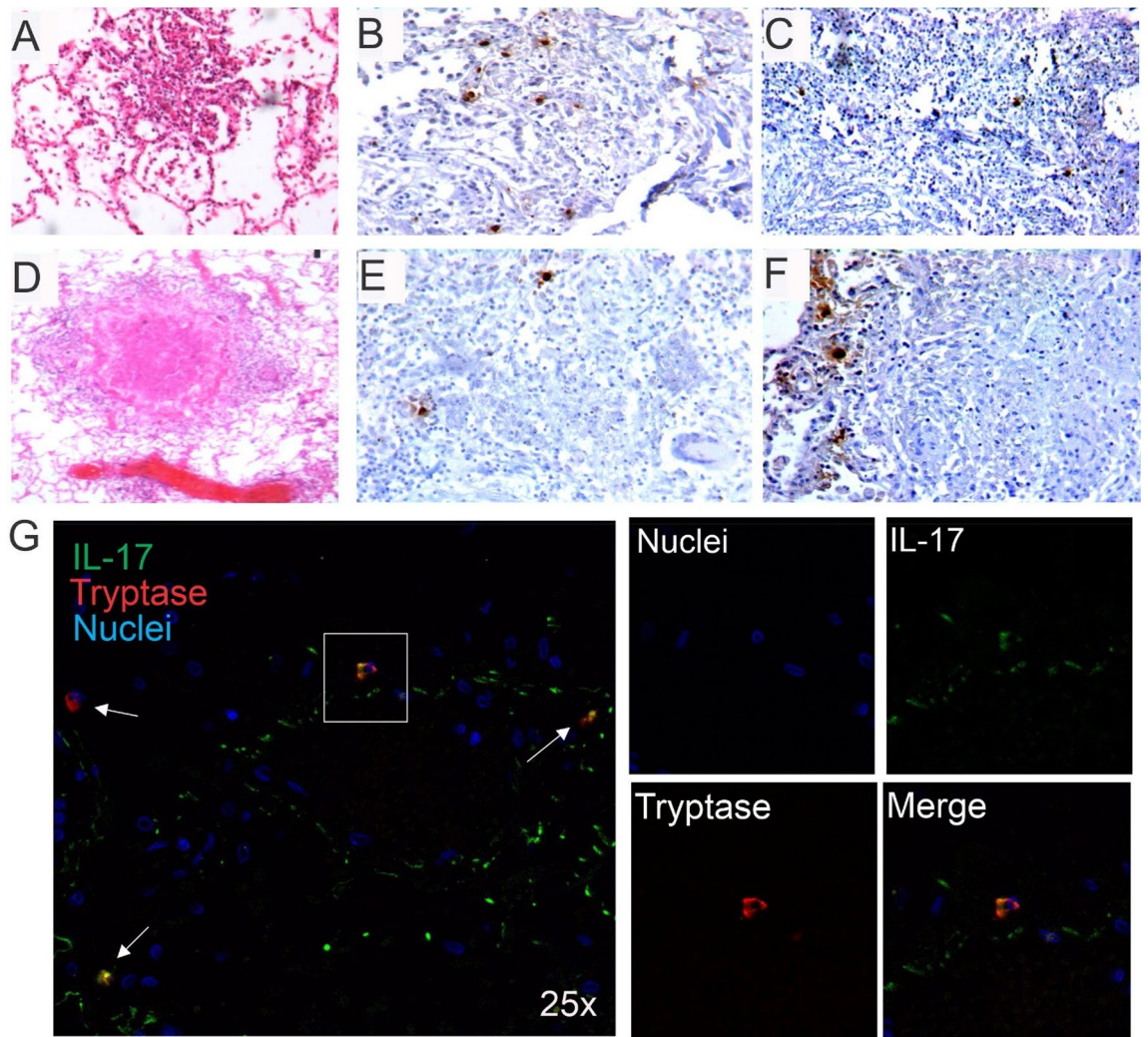


Figure 3. Mast cells are observed in granulomas and express IL-17A. Representative micrographs of different types of granulomatous lesions (incipient, mature or necrotic) were stained with HE or with anti-human anti-tryptase or anti-chymase immunoperoxidase antibodies to identify MC_T or MC_C. (A) Small incipient granuloma. Both MC phenotypes (B) MC_T and (C) MC_C are detected within the inflammatory area of incipient granulomas. (D) Mature granuloma with central necrosis. (E) MC_T and MC_C (F) are not infiltrating mature granulomas but both subtypes are observed in the periphery. Micrographs are representative of 11 TB necropsies. Representative section of incipient granuloma was incubated with anti-IL-17A (Alexa 488 label) and anti-tryptase antibodies (Alexa 647 label). (G) Low power micrograph shows numerous IL-17 + cells, and MC_T. High power micrograph of the inset shows MC_T staining positive for IL-17A.

periphery or close proximity in mature or necrotic granulomas. Since different immune cells including T lymphocytes are part of the granuloma structure, a direct interaction between MCs and T cells is likely to occur at this site. MC cytokines including IL-17, and TNF- α are necessary for granuloma maturation and maintenance in mouse TB infection⁴³. Although MC-TNF- α association was not observed (data not shown), we showed IL-17A positive MCs in the periphery of granulomas. Using an IL-17A gene-knockout mouse model, Okamoto-Yoshida et al. reported that IL-17A is necessary for granuloma maturation with $\gamma\delta$ T cells as the major IL-17 source⁴⁴. Also, granuloma formation was impaired in an IL-17A-deficient mouse model of sarcoidosis⁴⁵. Therefore, we would like to propose the concept that MCs contribute to the initial step of cellular recruitment at the infection site, remain outside the inflammatory core during the adaptive immune stage, and orchestrate granuloma maturation via IL-17 expression.

In severe and chronic TB infection, fibrosis is the result of excessive inflammation¹¹. MCs are abundant in fibrotic sites in non-infectious lung diseases⁴⁶, including idiopathic pulmonary fibrosis⁴⁷ and cystic fibrosis⁴⁸. In addition, MCs products such as the fibroblast growth factor 2 (FGF-2)⁴⁹, prostaglandin E2 (PGE2)⁵⁰, IL-1 β ⁵¹, TGF- β ^{10,52,53}, tryptase^{2223,54,55} and chymase^{47,56,57} are known to contribute to fibrogenesis^{50,53,58}. Our study reproduces findings described in idiopathic pulmonary fibrosis where MCs are increased in numbers and are partially degranulated at fibrotic sites^{46,59}. Furthermore, we found a switch in MC phenotype from MC_T to MC_{TC} in fibrotic areas. In line with this, Andersson et al., correlated high MC_{TC} numbers with lung function, tissue

References

1. Pezzella, A. T. History of pulmonary tuberculosis. *Thorac. Cardiovasc. Surg.* **29**(1), 1–17 (2019).
2. Sanyaolu, A. *et al.* Tuberculosis: A review of current trends. *EIJ* **3**, 000123 (2019).
3. Garcia-Rodriguez, K. M. *et al.* The role of mast cells in tuberculosis: Orchestrating innate immune crosstalk?. *Front. Immunol.* **8**, 1290 (2017).
4. de Martino, M. *et al.* Immune response to mycobacterium tuberculosis: A narrative review. *Front. Pediatr.* **7**, 350 (2019).
5. Ramakrishnan, L. Revisiting the role of the granuloma in tuberculosis. *Nat. Rev. Immunol.* **12**(5), 352–366 (2012).
6. Pagán, A. J. & Ramakrishnan, L. The formation and function of granulomas. *Annu. Rev. Immunol.* **36**, 639–665 (2018).
7. Shen, H. & Chen, Z. W. The crucial roles of Th17-related cytokines/signal pathways in *M. tuberculosis* infection. *Cell. Mol. Immunol.* **15**(3), 216–225 (2018).
8. Im, J. G. *et al.* CT-pathology correlation of pulmonary tuberculosis. *Crit. Rev. Diagn. Imaging* **36**(3), 227–285 (1995).
9. Subbian, S. *et al.* Lesion-specific immune response in granulomas of patients with pulmonary tuberculosis: A pilot study. *PLoS ONE* **10**(7), e0132249 (2015).
10. Nakayama, S. *et al.* Transforming growth factor β - and interleukin 13-producing mast cells are associated with fibrosis in bone marrow. *Hum. Pathol.* **62**, 180–186 (2017).
11. Wilson, M. S. & Wynn, T. A. Pulmonary fibrosis: Pathogenesis, etiology and regulation. *Mucosal. Immunol.* **2**(2), 103–121 (2009).
12. Johnzon, C.-F., Rönnerberg, E. & Pejler, G. The role of mast cells in bacterial infection. *Am. J. Pathol.* **186**(1), 4–14 (2016).
13. Gri, G. *et al.* Mast cell: An emerging partner in immune interaction. *Front. Immunol.* **3**, 120 (2012).
14. Krystel-Whittemore, M., Dileepan, K. N. & Wood, J. G. Mast cell: A multi-functional master cell. *Front. Immunol.* **6**, 620 (2016).
15. Hsieh, F. H. *et al.* Human airway epithelial cell determinants of survival and functional phenotype for primary human mast cells. *Proc. Natl. Acad. Sci. USA* **102**(40), 14380–14385 (2005).
16. Cruse, G. & Bradding, P. Mast cells in airway diseases and interstitial lung disease. *Eur. J. Pharmacol.* **778**, 125–138 (2016).
17. van den Boogaard, F. E. *et al.* Mast cells impair host defense during murine streptococcus pneumoniae pneumonia. *J. Infect. Dis.* **210**(9), 1376–1384 (2014).
18. Urb, M. & Sheppard, D. C. The role of mast cells in the defence against pathogens. *PLoS Pathog.* **8**(4), e1002619 (2012).
19. Bini, E. I. *et al.* The implication of pro-inflammatory cytokines in the impaired production of gonadal androgens by patients with pulmonary tuberculosis. *Tuberculosis* **95**(6), 701–706 (2015).
20. Seligson, D. *et al.* Expression of transcription factor Yin Yang 1 in prostate cancer. *Int. J. Oncol.* **27**(1), 131–141 (2005).
21. Erjefält, J. S. Mast cells in human airways: The culprit?. *Eur. Respir. Rev.* **23**(133), 299–307 (2014).
22. Abe, M. *et al.* Effect of mast cell-derived mediators and mast cell-related neutral proteases on human dermal fibroblast proliferation and type I collagen production. *J. Allergy Clin. Immunol.* **106**(1), S78–S84 (2000).
23. Cairns, J. A. & Walls, A. F. Mast cell tryptase stimulates the synthesis of type I collagen in human lung fibroblasts. *J. Clin. Investig.* **99**(6), 1313–1321 (1997).
24. Andersson, C. K. *et al.* Novel site-specific mast cell subpopulations in the human lung. *Thorax* **64**(4), 297–305 (2009).
25. Bradding, P. Human lung mast cell heterogeneity. *Thorax* **64**(4), 278–280 (2009).
26. Muñoz, S., Rivas-Santiago, B. & Enciso, J. A. Mycobacterium tuberculosis entry into mast cells through cholesterol-rich membrane microdomains. *Scand. J. Immunol.* **70**(3), 256–263 (2009).
27. Muñoz, S. *et al.* Mast cell activation by *Mycobacterium tuberculosis*: Mediator release and role of CD48. *J. Immunol.* **170**(11), 5590 (2003).
28. Chiba, N. *et al.* Mast cells play an important role in *Chlamydia pneumoniae* lung infection by facilitating immune cell recruitment into the airway. *J. Immunol.* **194**(8), 3840–3851 (2015).
29. Abraham, S. N. & St John, A. L. Mast cell-orchestrated immunity to pathogens. *Nat. Rev. Immunol.* **10**(6), 440–452 (2010).
30. Carlos, D. *et al.* Mast cells modulate pulmonary acute inflammation and host defense in a murine model. *J. Infect. Dis.* **196**(9), 1361–1368 (2007).
31. Sasindran, S. J. & Torrelles, J. B. Mycobacterium tuberculosis infection and inflammation: What is beneficial for the host and for the bacterium?. *Front. Microbiol.* **2**, 2–2 (2011).
32. Silva Miranda, M. *et al.* The Tuberculous Granuloma: An Unsuccessful host defence mechanism providing a safety shelter for the bacteria?. *Clin. Dev. Immunol.* **2012**, 139127 (2012).
33. Gallenga, C. E. *et al.* Interleukin-1 family cytokines and mast cells: Activation and inhibition. *J. Biol. Regul. Homeost. Agents* **33**(1), 1–6 (2019).
34. Conti, P. *et al.* Induction of pro-inflammatory cytokines (IL-1 and IL-6) and lung inflammation by Coronavirus-19 (COVI-19 or SARS-CoV-2): Anti-inflammatory strategies. *J. Biol. Regul. Homeost. Agents* **34**(2), 327–331 (2020).
35. Conti, P. *et al.* How to reduce the likelihood of coronavirus-19 (CoV-19 or SARS-CoV-2) infection and lung inflammation mediated by IL-1. *J. Biol. Regul. Homeost. Agents* **34**(2), 333–338 (2020).
36. Galli, S. J. & Gaudenzio, N. Human mast cells as antigen-presenting cells: When is this role important in vivo?. *J. Allergy Clin. Immunol.* **141**(1), 92–93 (2018).
37. Malaviya, R. *et al.* Mast cell phagocytosis of FimH-expressing enterobacteria. *J. Immunol.* **152**(4), 1907–1914 (1994).
38. Katsoulis-Dimitriou, K. *et al.* Mast cell functions linking innate sensing to adaptive immunity. *Cells* **9**, 12 (2020).
39. Stelekati, E. *et al.* Mast cell-mediated antigen presentation regulates CD8⁺ T cell effector functions. *Immunity* **31**(4), 665–676 (2009).
40. Ehlers, S. & Schaible, U. E. The granuloma in tuberculosis: Dynamics of a host-pathogen collusion. *Front. Immunol.* **3**, 411–411 (2013).
41. Tawevisit, M. & Poumsuk, U. High mast cell density associated with granulomatous formation in tuberculous lymphadenitis. *Southeast Asian J. Trop. Med. Public Health* **38**(1), 115 (2007).
42. Celasun, B., Crow, J. & Scheuer, P. J. Mast cells in granulomatous liver disease. *Pathol. Res. Pract.* **188**(1–2), 97–100 (1992).
43. Carlos, D. *et al.* TLR2-dependent mast cell activation contributes to the control of *Mycobacterium tuberculosis* infection. *Microbes Infect.* **11**(8), 770–778 (2009).
44. Okamoto Yoshida, Y. *et al.* Essential role of IL-17A in the formation of a mycobacterial infection-induced granuloma in the lung. *J. Immunol.* **184**(8), 4414–4422 (2010).
45. Jiang, D. *et al.* Inhibited IL-17A ameliorates sarcoid-like granulomatosis in mice. *Eur. Respir. J.* **46**(suppl 59), 3310 (2015).
46. Pesci, A. *et al.* Mast cells in fibrotic lung disorders. *Chest* **103**(4), 989–996 (1993).
47. Hirata, K. *et al.* Enhanced mast cell chymase expression in human idiopathic interstitial pneumonia. *Int. J. Mol. Med.* **19**(4), 565–570 (2007).
48. Andersson, C. K. *et al.* Activated MCTC mast cells infiltrate diseased lung areas in cystic fibrosis and idiopathic pulmonary fibrosis. *Respir. Res.* **12**(1), 139 (2011).
49. Inoue, Y. *et al.* Human mast cell basic fibroblast growth factor in pulmonary fibrotic disorders. *Am. J. Pathol.* **149**(6), 2037–2054 (1996).
50. Bradding, P. & Pejler, G. The controversial role of mast cells in fibrosis. *Immunol. Rev.* **282**(1), 198–231 (2018).
51. Conti, P. *et al.* IL-1 induces thromboxane-A2 (TxA2) in COVID-19 causing inflammation and micro-thrombi: Inhibitory effect of the IL-1 receptor antagonist (IL-1Ra). *J. Biol. Regul. Homeost. Agents* **34**(5), 1623–1627 (2020).

52. Yue, X., Shan, B. & Lasky, J. A. TGF- β : Titan of lung fibrogenesis. *Curr. Enzyme Inhibit.* **6**(2), 67 (2010).
53. Overed-Sayer, C. *et al.* Are mast cells instrumental for fibrotic diseases?. *Front. Pharmacol.* **4**, 174 (2014).
54. Bagher, M. *et al.* Mast cells and mast cell tryptase enhance migration of human lung fibroblasts through protease-activated receptor 2. *Cell Commun. Signal* **16**(1), 59–59 (2018).
55. Wygrecka, M. *et al.* Mast cells and fibroblasts work in concert to aggravate pulmonary fibrosis: Role of transmembrane SCF and the PAR-2/PKC- α /Raf-1/p44/42 signaling pathway. *Am. J. Pathol.* **182**(6), 2094–2108 (2013).
56. Tomimori, Y. *et al.* Involvement of mast cell chymase in bleomycin-induced pulmonary fibrosis in mice. *Eur. J. Pharmacol.* **478**(2), 179–185 (2003).
57. Matsumoto, T. *et al.* Chymase inhibition prevents cardiac fibrosis and improves diastolic dysfunction in the progression of heart failure. *Circulation* **107**(20), 2555–2558 (2003).
58. Hügle, T. Beyond allergy: the role of mast cells in fibrosis. *Swiss Med. Wkly.* **144**, 13999 (2014).
59. Groot Kormelink, T. *et al.* Immunoglobulin free light chains are increased in hypersensitivity pneumonitis and idiopathic pulmonary fibrosis. *PLoS ONE* **6**(9), e25392–e25392 (2011).
60. Rubinchik, E. & Levi-Schaffer, F. Mast cells and fibroblasts: Two interacting cells. *Int. J. Clin. Lab. Res.* **24**(3), 139–142 (1994).
61. Zhang, T. *et al.* Typical antimicrobials induce mast cell degranulation and anaphylactoid reactions via MRGPRX2 and its murine homologue MRGPRB2. *Eur. J. Immunol.* **47**(11), 1949–1958 (2017).
62. Bacci, S. & Romagnoli, P. Drugs acting on mast cells functions: A cell biological perspective. *Inflamm. Allergy Drug. Targets* **9**(4), 214–228 (2010).

Acknowledgements

The authors want to thank Orsolya Kiss and Mayra Silva Miranda for her support with fluorescent microscopy and Alejandro Lopez Saavedra together with the Advanced Microscopy Unit, INCAN, RAI, UNAM for their support using the confocal microscope.

Author contributions

K.M.G.R., R.H.P. and S.B.P. participated in the research design. Material preparation, data collection and analysis were performed by K.M.G.R. K.M.G.R. and E.I.B. conducted experiments. S.H.Y. produced micro-array tissues. K.M.G.R. and R.H.P. performed data analysis. The first draft of the manuscript was written by K.M.G.R. and R.H.P. and S.B.P. commented on previous versions of the manuscript. All authors revised and approved final version.

Funding

KMGR was supported by the National Council of Science and Technology (CONACYT) funding.

Competing interests

The authors declare no competing interests.

Additional information

Supplementary Information The online version contains supplementary material available at <https://doi.org/10.1038/s41598-021-89659-6>.

Correspondence and requests for materials should be addressed to R.H.-P.

Reprints and permissions information is available at www.nature.com/reprints.

Publisher's note Springer Nature remains neutral with regard to jurisdictional claims in published maps and institutional affiliations.



Open Access This article is licensed under a Creative Commons Attribution 4.0 International License, which permits use, sharing, adaptation, distribution and reproduction in any medium or format, as long as you give appropriate credit to the original author(s) and the source, provide a link to the Creative Commons licence, and indicate if changes were made. The images or other third party material in this article are included in the article's Creative Commons licence, unless indicated otherwise in a credit line to the material. If material is not included in the article's Creative Commons licence and your intended use is not permitted by statutory regulation or exceeds the permitted use, you will need to obtain permission directly from the copyright holder. To view a copy of this licence, visit <http://creativecommons.org/licenses/by/4.0/>.

© The Author(s) 2021